remote sensing

MDPI

Article

Holocene Erosional Processes in a Highly Exposed Intertidal Sandstone Reef Inferred from Remote Sensing Data

Nicolás Ferrer [1,*], Kella Santana [2], Javier Martín [1], José Valdazo [2] and Oscar Bergasa [2]

[1] Instituto de Oceanografía y Cambio Global, University of Las Palmas de Gran Canaria (IOCAG-ULPGC), Parque Científico Tecnológico Marino de Taliarte, s/n., 35214 Telde, Spain; javier.martin@ulpgc.es
[2] Elittoral Estudios de Ingeniería Costera y Oceanográfica SLNE, Edificio Polivalente II, Parque Científico Tecnológico, Campus Universitario de Tafira, 35017 Las Palmas, Spain; ksantana@elittoral.es (K.S.); jvaldazo@elittoral.es (J.V.); obergasa@elittoral.es (O.B.)
* Correspondence: nicolas.fvg@ulpgc.es

Abstract: An intertidal sandstone reef, named *barra* de Las Canteras, protects the western coast of Las Palmas de Gran Canaria city (Canary Islands, Spain). The beach-reef system of Las Canteras constitutes one of the most valuable coastal geomorphological sites in the archipelago. Stratigraphic studies have identified the formation of the reef in the Last Interglacial (MIS 5e) in a coastal sedimentary paleo-environment. The rock structure is highly exposed to the Atlantic swell and consists mainly of a sandstone beachrock with a medium resistance to erosional processes. However, the historical and current erosion rates and the original extent of the reef are not known to date. This paper explores the geomorphological structure of the reef by combining a topo-bathymetric analysis (obtained by differential GPS, multibeam echosounder and hyperspectral sensor) and the analysis of geomorphological features on high-resolution images, obtained with a hyperspectral camera mounted on a UAV. The results provide a comprehensive, high-resolution image of the subaerial and submerged morphology of the reef. The structure reflects the distribution of erosional fronts and the existence of collapsing submarine blockfields and nearshore, uneroded, remnant reliefs. Detailed analysis of these features allows to estimate the probable original extent of the sandstone reef and to relate the erosional retreat processes to the sea-level dynamics during the Holocene.

Keywords: sandstone reef; beachrock; coastal erosion; Las Canteras; Canary Islands

check for updates

Citation: Ferrer, N.; Santana, K.; Martín, J.; Valdazo, J.; Bergasa, O. Holocene Erosional Processes in a Highly Exposed Intertidal Sandstone Reef Inferred from Remote Sensing Data. *Remote Sens.* **2023**, *15*, 2968. https://doi.org/10.3390/rs15122968

Academic Editor: Paolo Ciavola

Received: 10 April 2023
Revised: 29 May 2023
Accepted: 5 June 2023
Published: 7 June 2023

Copyright: © 2023 by the authors. Licensee MDPI, Basel, Switzerland. This article is an open access article distributed under the terms and conditions of the Creative Commons Attribution (CC BY) license (https://creativecommons.org/licenses/by/4.0/).

1. Introduction

Sandstone reefs are important paleoenvironmental markers and natural protectors against erosion in tropical coastal regions [1]. Despite their ecological importance, they have received much less scientific attention than other similar formations, such as coral reefs [2]. The intertidal sandstone reefs of northeastern Brazil are probably the best known and most studied in the world [1,3,4]. In the State of Pernanmuco, intertidal beachrocks crops out parallel to the coast for tens of kilometers. They are mostly composed of parallel stratified layers of calcarenites with 4–5° seaward dips, to which a Holocene age is attributed [4,5]. Their unusual development in this part of the world has motivated their valuation as important geoheritage and geotourism elements [1,6,7]. A remarkable subtropical sandstone reef also occurs in the Canary Islands. The sandstone reef of Las Canteras is up to six meters thick and has subhorizontal parallel laminations that dip gently seaward, so it has been identified as a beachrock formation [8,9]. The sandy grains are strongly compacted by carbonate cement and contain abundant remains of marine organisms, mainly mollusks, algae and foraminifera [10]. Due to its stratigraphic similarity with other sandstone outcrops and marine conglomerates of the eastern Canaries, it has traditionally been considered part of a larger sedimentary unit called Terraza Baja de Las Palmas [11] or Rasa Jandiense [12], dated to the Last Interglacial MIS 5e.

In many coasts, natural reefs are interposed offshore, safeguarding the sedimentary stability of the sandy beaches [13,14]. Rocky and erosional coastal environments support sedimentary deposits and beaches of very diverse characteristics, controlled by complex geological structures and their erosion-deposition dynamics [15]. According to Gallop et al. [16], the existence of rock controls, rather than being infrequent, is the rule on sandy beaches on coasts worldwide. Several studies have pointed out the determinant influence of hard rock structures, such as reefs, headlands or underlying outcrops, on the morphodynamics of sandy beaches [16–20]. They act as protectors against coastal erosion, generating strong energy gradients between exposed and protected sectors [18,21]. Inherited geological structures introduce complexity into wave-breaking patterns, currents and sedimentary dynamics, cross-shore and alongshore, causing mismatches between theoretical morphodynamic models and the actual beach morphologies observed in the environments [22].

A complete understanding of the morphodynamic behavior of rock-controlled coastal systems requires a simultaneous examination of subaerial and subaqueous geomorphic transformations. Topo-bathymetric studies have become frequent, especially in the monitoring of rapid response sedimentary systems, such as beaches [20]. The monitoring of the submerged surfaces presents a greater technical challenge than the monitoring of land surfaces. Traditional techniques have used boat-borne echosounders [23,24], but high costs often do not allow for high-recurrence surveys and they are not operational in shallow intertidal areas. The need for more versatile and less expensive alternative techniques has led to the development of bathymetric procedures, such as video monitoring [20,25] or hyperspectral sensing [26,27]. The results of these new techniques have generally proved to be reliable and represent new tools for research.

Reefs can dissipate much of the incident wave energy on coasts [28,29], which triggers erosion on reef structures, especially during storm events. The progressive erosion of tropical and subtropical sandstone reefs can produce a chain of very negative socio-ecological consequences. From the loss of the ecosystem services linked to the natural protection of the reefs, a drastic alteration of the hydrodynamic regime and a serious impact on beach morphology and marine ecosystems can be expected. Despite the important geodynamic implications, especially for the configuration and geomorphological stability of many sedimentary coasts, the erosion of highly exposed rocky reefs is a poorly investigated phenomenon to date. From the knowledge of the morphodynamics of rocky shores, we know that coastal rock platforms are dynamic and eroded by mechanical and abrasive wave action, as well as by other physical, chemical and biological weathering processes [30,31]. Shore platforms are primarily eroded in two ways: by a progressive micro-erosional lowering [32–35] and by sporadic, larger block detachments usually deposited on the upper platform and reworked by storm waves [36–38]. Moreover, although the movement of non-cohesive sediments can occur at greater depths, erosion of solid rock by waves is strongly concentrated in the break zone, near the still waters and intertidal zone [39–42].

The planning of conservation actions to avoid the future degradation of relevant natural elements such as sandstone reefs, requires a better understanding of the magnitude and forms of past and present erosional processes. In order to contribute to this knowledge, the aim of this work was to obtain, through a combination of different instruments and remote sensing techniques, a high-resolution topo-bathymetric model of the largest sandstone reef of the Canary Islands (the reef of Las Canteras), which provides new insights into its possible original configuration and spatio-temporal evolution. The article contains the area description and the acquisition methodology of a high-resolution topo-bathymetric model of the reef of Las Canteras, combining GPS, echosounder and hyperspectral sensing. The results include a comprehensive analysis of morphometric features, geomorphological units and active processes on the reef. The discussion finally provides an evolutionary and contextualized interpretation of the reef of Las Canteras based on the observations.

2. Study Area

The sandstone reef of Las Canteras is located in the city of Las Palmas de Gran Canaria (Canary Islands, Spain), at a subtropical latitude of the eastern Atlantic Ocean (~28°N and ~15°W), off the coast of Africa (Figure 1a). The reef is popularly known as *la barra* ('the bar') and is divided into six sections [43]. *La barra grande* is the largest fragment and the most relevant in respect to coastal hydrodynamics and sediment transport [44]. It runs parallel to the beach at a distance from the shore of about 200 m, has an approximate length of 850 m and an average intertidal width of 50 m (Figure 1b). *La barra* protects Las Canteras beach from the North Atlantic swell, which in this sector has an average significant height of 1.5 m and a peak period of more than 10 s. The storm waves reach significant heights of more than 4 m [21,45]. The morphodynamics of the different sectors of Las Canteras beach and its sedimentary stability is highly conditioned by the natural protection of *la barra* [21,45–50]. In the most protected coastal sector, normal wave overtopping barely exceeds the reef at low tide, generating an intermediate semi-enclosed coastal lagoon with high-marine biodiversity [51,52]. Likewise, during storm surges, *la barra* prevents the cross-shore transport of sediments offshore, converting the intermediate shallow seabed into a sand reservoir for the beach.

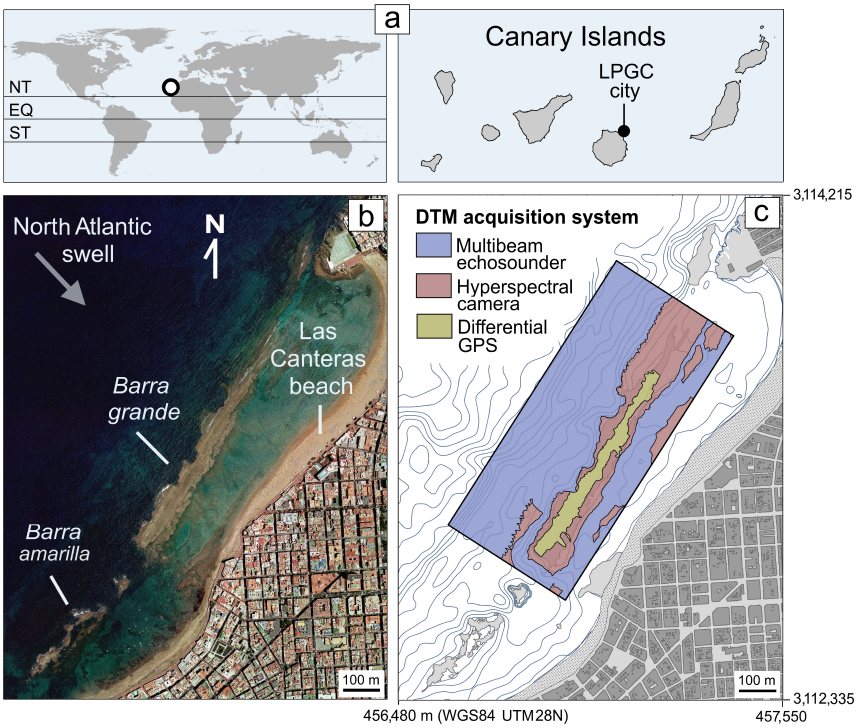

Figure 1. (**a**) Geographical location of *la barra* de Las Canteras, in the Canary Islands (LPGC stands for the city of Las Palmas de Gran Canaria). NT, Northern Tropic, EQ, Ecuator, ST, Southern Tropic. (**b**) Distribution of the main fragments of the reef (*barra grande* and *barra amarilla*) on digital orthophoto at low tide (IDE Canarias, GRAFCAN). (**c**) Zonation of the technological systems used for the acquisition of the digital topo-bathymetric model of *la barra grande*.

It can be assumed that the stratified sandstone reef of *la barra* has average levels of resistance to coastal erosion. However, as no empirical data exist, we do not know the patterns, magnitudes and rates of erosion to which it is subjected to in the short, medium and long term. The degradation of the sandstone reef of Las Canteras may lead to the degradation of the beach it protects, which in turn is one of the most important tourist elements of Las Palmas de Gran Canaria city, that is, of the main economic and demographic center of the Canary Islands.

3. Materials and Methods

3.1. GPS Topography

The topographic surfaces of the upper part of *la barra*, from 0 m above mean sea level (m asl), were obtained in 2019, by carrying on foot, at low tide, a differential GPS configured in kinematic mode to receive altimetry data every 50 cm (Figure 1c). The topographic instrument is a Topcon HiperV model, which receives positions from the GPS and GLONASS satellite constellations, and received real-time kinematic (RTK) corrections, via internet (mobile telephony), through NTRIP protocol from the GRAFCAN Permanent Stations service (https://www.grafcan.es/red-de-estaciones, accessed on 15 January 2019). The device manufacturer defines a spatial accuracy for RTK in kinematic mode of 10 mm + 1 ppm in the horizontal dimension and 15 mm + 1 ppm in the vertical dimension. More than 70,000 altimetry values with xyz coordinates of the upper part of *la barra grande* were obtained from the GPS topography.

3.2. Multibeam Bathymetry

Seabed surfaces around *la barra*, below −1.5 m asl, were obtained in 2019 (simultaneous to GPS topography) by on-board multibeam echosounder, at 3 knots maximum speed at high tide (Figure 1c). The system consists of a NORBIT iWBMS echosounder that emits 256 fan-shaped beams covering an angle of 160°. The direct measurement of sound speed was calculated using data collected by a Valeport Swift-plus profiler. The system was completed by integrated Applanix Wavemaster inertial motion sensors and an Applanix navigation system using Trimble technology. An eight-core, high-capacity computer with HYSWEEP software, synchronized and integrated the data received from all system components: multibeam echosounder, positioning system, heading, motion, tide and sound speed sensors. Post-processing by Patch test calibration, velocity profiling and denoising was performed using Hypack's MBMAX software. After post-processing steps, a regular grid of xyz bathymetric points of the underwater surrounding environment was obtained every 50 cm.

3.3. Hyperspectral Altimetry

High-resolution aerial images were obtained in 2020 using a RESONON Pika L hyperspectral camera attached to a drone with a gimbal system and irradiance sensor (Figure 1c). The camera has a spectral range of 400–1000 nm and a maximum spectral resolution of 2.1 nm. The flights were performed at an altitude of 120 m, following zig-zag trajectories with a spacing of 25 m. Radiometric and geometric correction was performed with SpectrononPro software, using calibration files to convert digital values. The orthophotos were mosaicked using the OrfeoToolbox. The specular reflections of the water were corrected using a *deglinting* algorithm [53] and the anomalous effects generated by the wave foam were corrected using an *inpainting* algorithm [54]. The subaerial part of the image was obtained at a final resolution of 10 cm, while a resolution of 30 cm in the submerged part was adopted to reduce the high-computational expense of solving the equations of the coastal water inversion involved in obtaining the bathymetry.

Bathymetry was obtained using radiative-transfer modelling of seawater in coastal environments. The inherent radiative effects of water, such as absorption and backscattering and the effects of light reflection at the bottom, were modelled in each of the hyperspectral bands, considering the different benthic covers. The model follows the semi-analytical form of the radiative transfer equations (RTE) [55], where the modelled reflectivity in a channel is obtained from the sum of the above factors. Calculating the surface reflectivity involves systems of non-linear equations that are impossible to solve analytically, so we used the Levenberg–Marquardt optimization algorithm [56]. It makes it possible to find the most suitable result by iteratively minimizing the error in respect to the reflectivity obtained by the sensor, applying cost function and minimal epsilon error. This algorithm provides very adequate results for this complex problem and uses moderate computational resources

compared to other algorithms. The resulting terrain model had a horizontal resolution of 1 m.

3.4. Detection of Active Processes

The detection of active erosional processes from 1954 to 2022 was carried through an exhaustive examination of historical aerial images of the extensive photo library of the Spatial Data Infrastructure (SDI) of the Canary Islands (GRAFCAN S.A., Canary Islands Government, https://www.idecanarias.es/, accessed on 10 February 2023). It contains 22 photograms between 1954 and 2000, with an almost biannual frequency, and 18 orthophotos between 2000 and 2022, with an almost annual frequency. Conventional aerial photographs from the 1950s to the 1990s have scales between 1:5000 and 1:25,000, and were georeferenced in the WGS84 UTM28N coordinate system. The digital orthophotos from the 2000s have resolutions varying between 12.5 and 50 cm/pixel and are available for GIS viewing via the Web Map Service. The detection of active processes was completed with field surveys at the outer edge of the reef.

3.5. Data Integration and Interpretation

GPS altimetry, composed of more than 70 thousand topographic point coordinates, and echosounder altimetry, composed of more than 1 million bathymetric point coordinates, were integrated into ArcGIS software under a WGS84 UTM28N reference system. The point cloud was used to construct an interpolation grid based on a triangle irregular network (TIN) and its subsequent conversion into a 50 cm resolution raster digital terrain model (DTM). Intertidal areas with no GPS or echosounder data were covered by the 1 m resolution hyperspectral sensor-derived DTM. The resulting digital model covers an area of interest of 380,000 m^2 including *la barra grande* and its nearby underwater environment up to 200 m away (Figure 2).

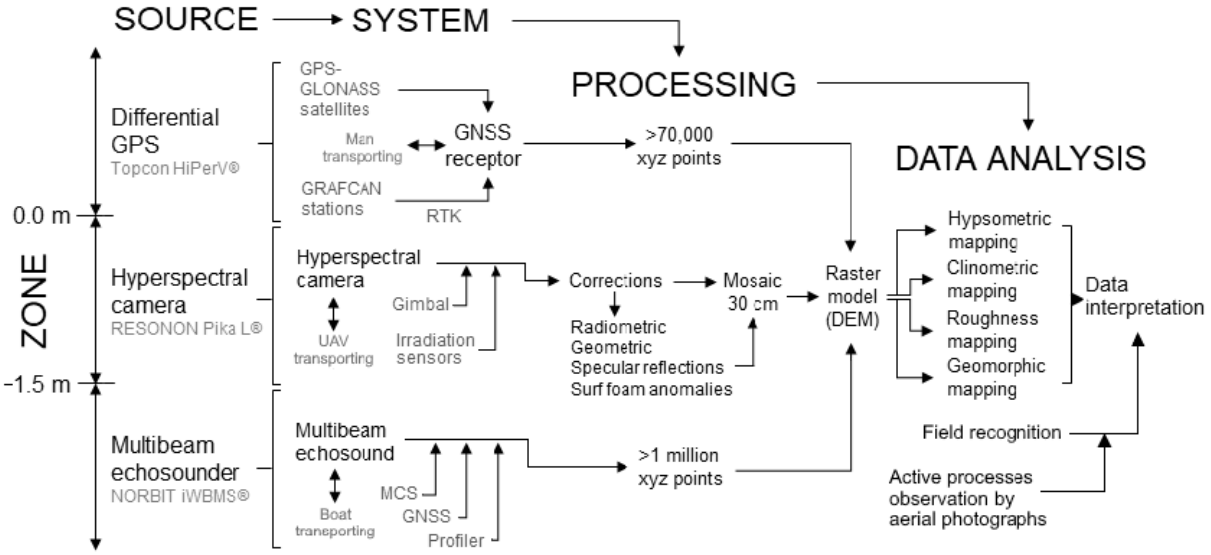

Figure 2. Workflow for the acquisition of topo-bathymetric data, integration into a digital topo-bathymetric model and the geomorphological interpretation of the rocky structure of *la barra grande* (Las Palmas de Gran Canaria, Canary Islands).

The concluding analysis of the digital topo-bathymetric model included two levels (Figure 2). At the first level, the morphometric structure was analyzed through GIS geoprocessing algorithms in order to examine the spatial distribution of altimetric ranges, terrain slopes and surface roughness. Terrain irregularity was calculated using the Vector Ruggedness Measure (VRM) [57,58]. This method measures terrain irregularity as the dispersion of the orthogonal vectors orientation of the grid cells within a raster neighborhood. At

the second level of analysis, geomorphological features were recognized combining the morphometric variables with the active processes detected on aerial photographs and the field recognition. Finally, geomorphological units were established to interpret evolutionary processes in the reef.

4. Results

4.1. Morphometric Structure

The morphometric structure entails a strictly morphological description of the surface features based on measured variables. The morphometric of *la barra* has been determined by analyzing the distribution of terrain altimetry, slopes and roughness.

The hypsometric structure (Figure 3a) of *la barra grande* comprises intertidal and subtidal sections. The surface of the main sandstone bank lies entirely in the regional tidal range of the Canary Islands, between −1.5 m asl at maximum low-spring tide, and 1.5 m asl at maximum high-spring tide. However, most of this area, approximately 60,730 m^2, is in the middle to lower intertidal zone, between −1 and 0 m asl. Only a few inner sectors of the sandstone surface, totaling a small extension of 2665 m^2, are developed above 0 m asl, and only in two small topographic outcrops of 12 m^2 each, which are located further inland, the elevations exceed 0.5 m asl. One of them reaches 0.68 m asl, which is the maximum altitude of the topo-bathymetric model. In between, there is a relatively extensive intertidal rocky surface of 14,425 m^2, whose elevations of between −0.5 and 0 m asl determine that it is slightly depressed in respect to the two previous surface bands.

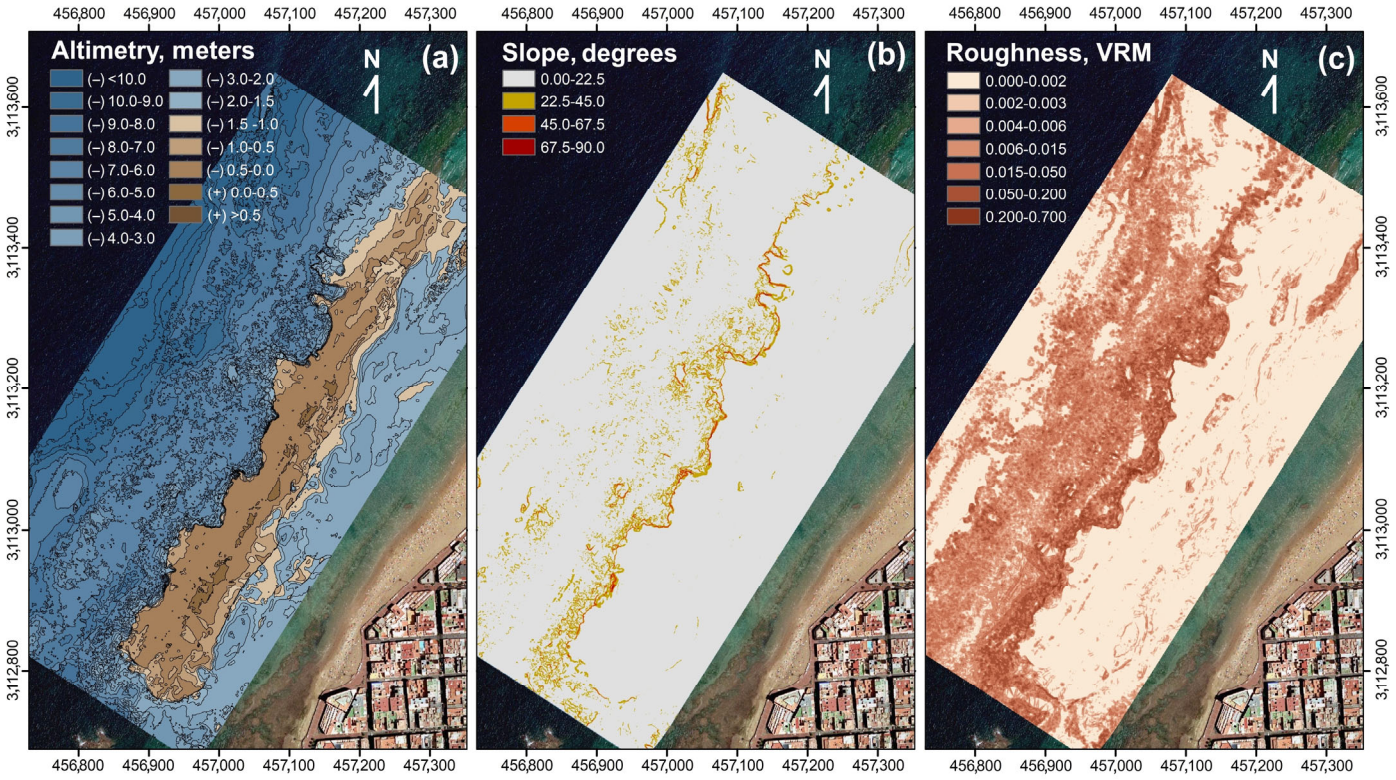

Figure 3. Morphometric variables derived from the digital topo-bathymetric model of *la barra grande* de Las Canteras (maps in metric units of the WGS84-UTM28N system) (**a**) distribution of altimetry and depths (meters); (**b**) distribution of terrain slopes (degrees); (**c**) distribution of terrain roughness (VRM = 0, completely smooth; VRM = 0.7, very rough).

At the seaward outer edge of the reef, the surface changes from intertidal depths of 0 to −1 m, to mean subtidal depths of −5 m. From the subtidal depths, towards offshore, a shallow underwater surface develops, reaching on average a depth of 12 m at a distance of 200 m from the outer edge of the reef. Above it, at least three small subtidal surfaces

are clearly distinguishable with prominences of 2 to 3 m in relation to their underwater surroundings (Figure 4). The first is 45 m from the outer nearest edge of the reef, has a top surface at a mean depth of −3.5 m and is surrounded by seabed surfaces of −5 to −6 m depth. The second is 50 m from the nearest outer edge, has a top surface at a mean depth of −2.8 m and is surrounded by submarine surfaces of −6 m depth. Additionally, the third is 100 m from the nearest reef edge, has a top surface at a mean depth of −4.5 m and is surrounded by average depths of −7 m.

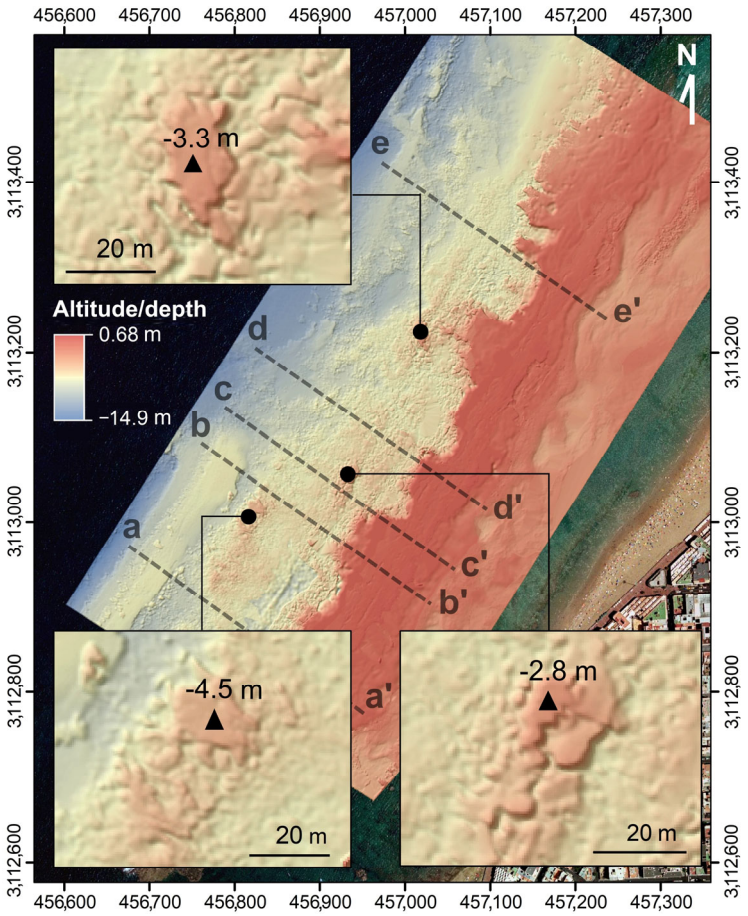

Figure 4. Topographic outcrops on the surrounding offshore seabeds, visible in the digital topo-bathymetric high-resolution model, and the surface roughness profiles of Figure 5 in dashed lines and letters (units in meters of the WGS84-UTM28N system).

The clinometric structure of the topo-bathymetric model of *la barra grande* shows significant zone differentiation (Figure 3b). Above −0.5 m asl, the surfaces are practically flat, although slightly trending NW (i.e., towards offshore) across planes with an average slope of less than 2 degrees. From the intertidal level of −0.5 m asl, the reef slope increases seaward. In some sectors, from −0.5 m asl, planes of variable cross-shore width between 25 and 50 m are observable, with slopes of up to 5 degrees to NW gradually penetrating the lower intertidal and subtidal zone of the water column and connecting the upper surface of the reef with the outer shallow subtidal seabed through small escarps of 1 to 2 m. In the sectors where these gently sloping surfaces are not developed, the almost flat surface of the reef top ends abruptly in the outer edge, in vertical 5–6 m cliffs which fall directly to the subtidal seabed. From here seaward, the outer seabed develops as a wide, low-slope surface, lying 1 to 2 degrees to the NW. In short, the topo-bathymetric model is dominated by flat or slightly sloping surfaces to the NW, except a line of steep slopes in the form of vertical escarpments of 1 to 6 m in height developed along the entire outer seaward-edge of the reef.

According to the observation of the topo-bathymetric model at a scale of 5 m, the surface irregularity, estimated using the VRM indicator, also marks significant spatial zonation in the surfaces of *la barra grande* and its submarine surroundings (Figure 3c). The upper intertidal surface of the reef is essentially smooth at this scale, with values very close to 0.0, that is the minimum roughness value of the VRM index. Additionally, essentially smooth are the inner subtidal seabeds, which lie between the sandstone reef and the present-day beach, at an average depth of −3 m. However, surface roughness increases dramatically on the outer subtidal-marine bottoms, starting from maximum values in the area adjacent to the outer edge of *la barra* and progressively decreasing (Figure 5). Maximum values occur in the areas adjacent to the outer reef escarpments, where values of up to 0.7 are reached (being 1.0 the theoretical maximum roughness value of the VRM index). The irregularity of the seabed decreases progressively towards the outside, as we move away from the edge of *la barra*, until, at a maximum distance of 150 m and −10 m depth, the high values of irregularity at an observation scale of 5 m practically disappear.

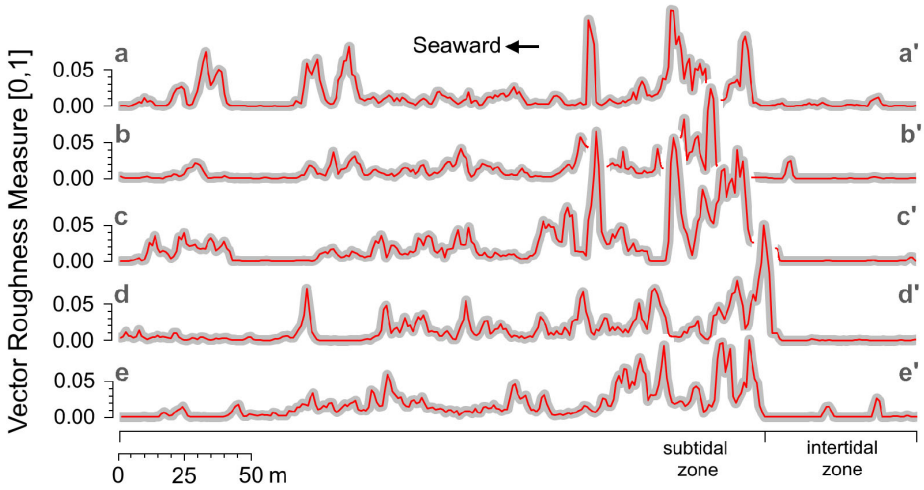

Figure 5. Vector Roughness Measure profiles showing the essentially smooth character of the intertidal zone, the very high surface irregularity of the subtidal zone adjacent to the outer seaward reef edge and the decreasing roughness towards offshore. The profile locations for letters a–e and a'–e' can be found in Figure 4.

4.2. Geomorphological Units

Geomorphological units are morphometrically similar features linked to a common forming processes. The morphometric results and subsequent field reconnaissance has made it possible to distinguish seven main geomorphological units in *la barra grande* of Las Canteras (Figure 6). The morphogenetic character of these units provides a spatio-temporal evolutionary interpretation, in which erosion processes play a primordial role.

Firstly, the reef currently shows a top platform of 50 m average width (U1, Figure 6), with abundant development of microerosional landforms (rills, potholes, ridges, etc.), as a product of the intense daily physical, chemical and biological weathering in the middle and upper intertidal zone (Figure 7). However, according to the roughness values, this platform is essentially smooth at the metric scale of the topo-bathymetric model. It develops from the lower limit of the middle intertidal zone to the upper intertidal zone at its inner landward edge. A drop of approximately 1 m between the inner and outer edge of the top platform determines the existence of a gentle slope towards the NW of between 1 and 2 degrees. However, it also declines in a NNE direction of less than 1 degree, determining the gradual lowering of *la barra grande* to subtidal depths at its northern end. An inner fringe of this top platform is topographically discordant with the rest of the surface, being sunk between 0.5 and 1 m from its natural level (Figure 7). This is due to the extraction, throughout the 18th and 19th century, of the calcareous sandstones of *la barra* for different urban uses in the city of Las Palmas de Gran Canaria (U2, Figure 6). However, three preserved remnants of the

mining activities (U3, Figure 6) show that the elevation of the inner edge was naturally at about 0.5 m asl, allowing the original pre-mining surface to be projected and reconstructed.

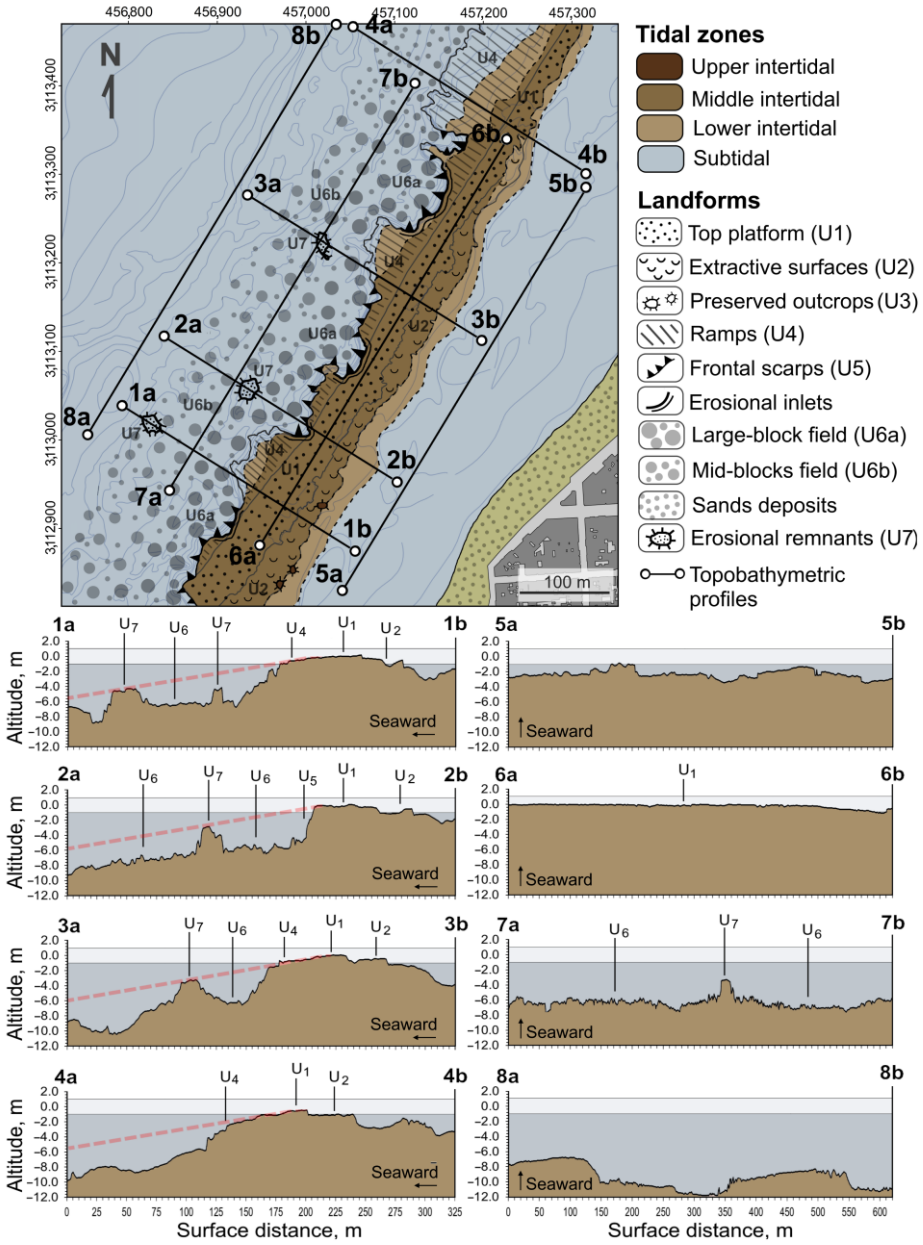

Figure 6. Geomorphological map with transverse (1a–1b to 4a–4b) and longitudinal (5 to 8) topobathymetric profiles (units in meters of the WGS84-UTM28N system). Geomorphological units: U1; intertidal top platform; U2, extractive depression surfaces; U3, preserved rocky outcrops; U4, intertidal ramps; U5, frontal escarpments; U6, submarine blockfields; U7, erosional remnants. The dotted lines represent the seaward projection of the intertidal ramps (U4) with 2–3 degrees of inclination, showing their theoretical connection with the erosional remnants (U7).

The outer edge of the top platform is planimetrically sinuous. The headlands are intertidal ramps (U4, Figure 6) of variable widths of between 25 and 50 m, with average slopes of approximately 5 degrees to the NW. On its surface, there are abundant parallel erosional rills visible in the field as a result of the mechanical action of the waves run-up at low tide (Figure 7). The intertidal ramps gradually penetrate the water table, ending in small subtidal escarpments (Figures 7 and 8). Between headlands, the inlets are incipient erosional corridors as a result of the retreat of the intertidal ramps by wave action. Instead

of ramps, we observe receding concavities in the inlets (Figure 7), where the outer edge of the top platform ends in vertical cliffs of greater height. Ultimately, the outer edge of the reef is steep, but the height of the frontal escarpments (U5, Figure 6) varies from 2 to 6 m depending on the intensity or magnitude of marine erosional retreat, which is deduced from the degree of planview penetration in the concavities (erosion) or the degree of prominence of the intertidal ramp-like headlands (preservation).

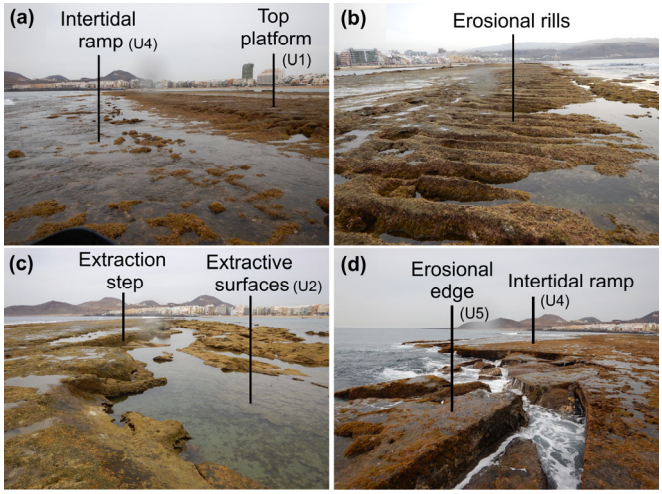

Figure 7. Photographs of intertidal geomorphological units: (**a**,**b**) intertidal top platform (U1, Figure 6) and ramps (U4, Figure 6) with erosional micromorphologies of weathering and parallel rill erosion; (**c**) extractive depressions (U2, Figure 6); (**d**) erosional edge and top of frontal escarpments (U5, Figure 6). Photographs are north-facing, except for (**b**), which is south-facing.

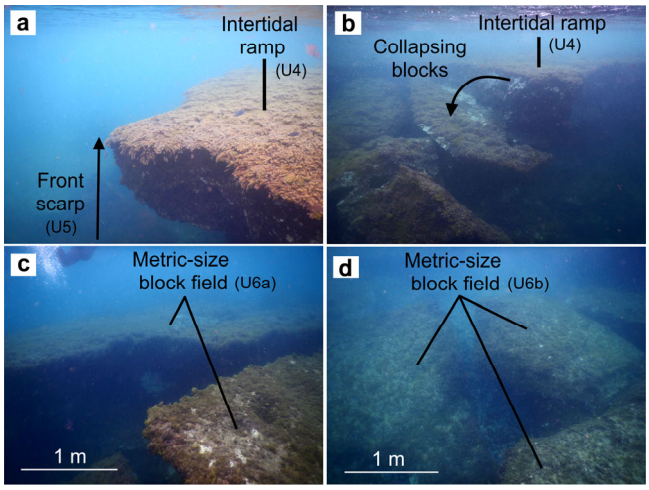

Figure 8. Photographs of subtidal geomorphological units: (**a**) outer section of an intertidal ramp (U2, Figure 6) ending in a frontal escarpment (U4, Figure 6); (**b**) collapsing blocks on the frontal walls of the intertidal ramp; (**c**,**d**) metric-sized blocks on the seabed adjacent to the outer reef edge (U6a, Figure 6). Scale of the photographs (**c**,**d**) is approximate.

At subtidal depths towards open water, the submarine platform is shallow with a gentle slope to offshore and very high surface roughness at the scale of the digital topo-bathymetric model. The analysis of the hyperspectral images together with the field inspections allowed to verify that this roughness corresponds to the presence of an extensive field of large sandstone blocks (U6). It extends up to a distance of approximately 150 m and up to −10 m in depth from the outer edge of the intertidal top platform (Figure 8). As can be deduced from their spatial distribution and composition, the blocks are the product

of detachments from the outer reef front (Figure 8). In other words, they result from the successive collapses and rockfalls that have taken place in the sandstone wall during the retreat caused by mechanical wave erosion.

The size of the rock fragments in the blockfield decreases with distance from the outer edge of the intertidal platform (Figure 5). A first submarine zone of width of 50 m (U6a, Figure 6) of more modern and larger rockfalls, runs parallel to the outer edge, and can be distinguished from a second submarine zone of 100 m width (U6b, Figure 6) of older and smaller collapsing blocks. The detection of seabed features in the high-resolution hyperspectral images allowed to establish a statistical estimate of the size of the blocks in the shallow submarine blockfield adjacent to the edge of the intertidal platform (U6a) (Figure 9). According to these results, about 60% of the blocks have surface sizes between 5 and 25 m^2; almost 20% have sizes between 25 and 125 m^2; and some blocks are larger than 125 m^2.

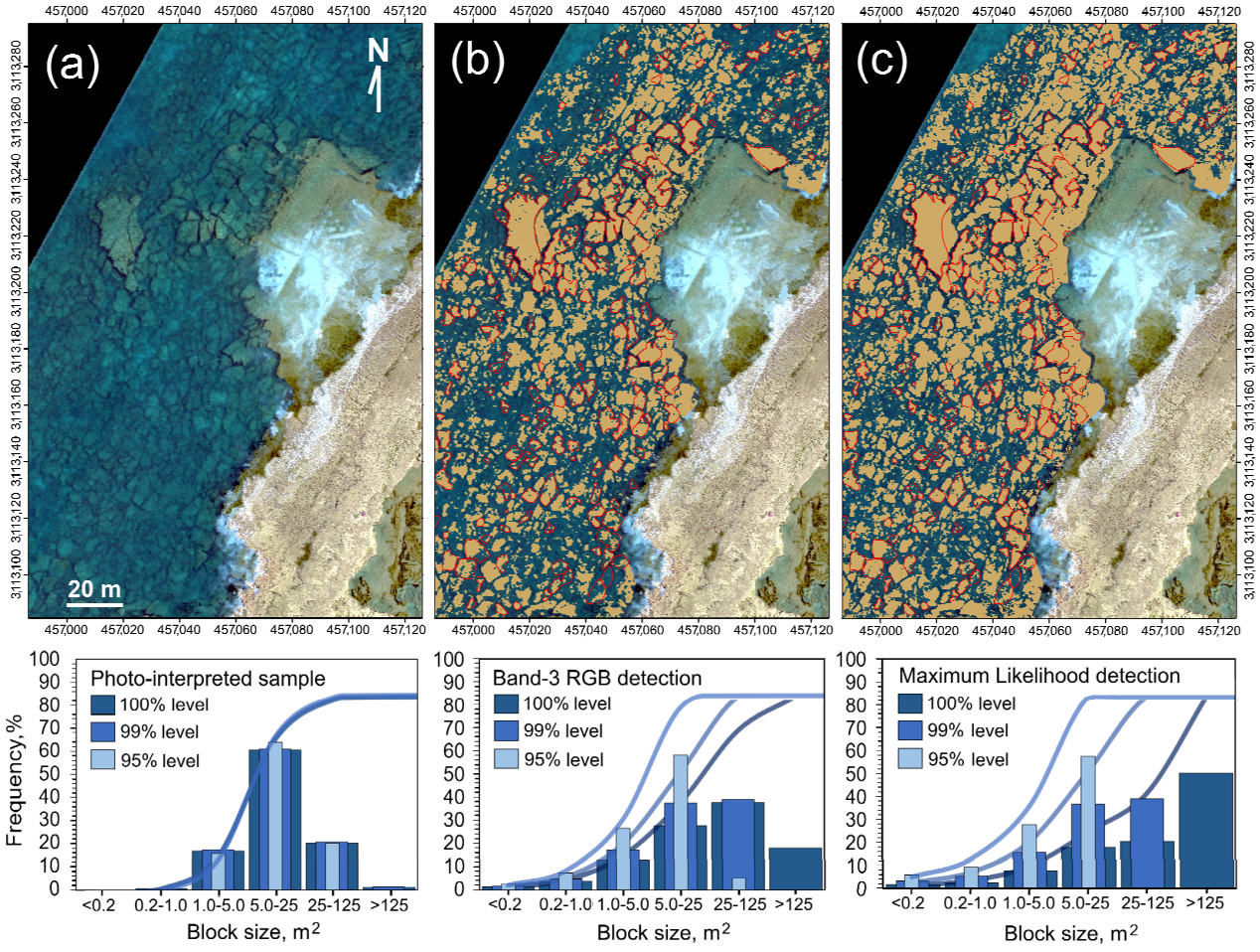

Figure 9. Blockfield on the near seabeds adjacent to the outer reef edge (WGS84-UTM28N units in meters) (**a**) High-resolution hyperspectral RGB image. (**b**) Blocks detection by light slicing in the green RGB band (brown) compared to the recognition by direct photo-interpretation at 590 random points (red contours). (**c**) Block detection by maximum likelihood algorithm from 822 RGB signature samples (brown) compared to direct photo-interpretation at 590 random points (red contours). The histograms show the distribution of the surface size of the blocks according to the three detection methods, considering 100%, 99% and 95% of the size distribution obtained.

In the middle of the blockfield originated by the marine erosional dismantling of the reef, the topo-bathymetric model showed the existence of topographic outcrops (Figure 4) interpretable as erosional remnants of *la barra* de Las Canteras (U7, Figure 6). The morpho-metric structure of these three rocky remnants allows to assimilate them with non-eroded

surfaces of *la barra*, which would have been separated from the main calcareous sandstone mass during its dismantling and erosional retreat over time. Therefore, the erosional remnants can be considered as key geomorphological indicators of the original extension of *la barra* and of the total longitudinal magnitude of its erosional retreat. The first is located 100 m from the outer edge of *la barra* (X.456825, Y.3113020, in UTM28N) and has a flat surface of 270 m^2; the second is located 50 m from the outer edge (X.457015, Y.3113220) and has a flat, more fragmented surface of 220 m^2; and the third is located ~40 m away (X.456935, Y.3113060) and has a flat surface of 130 m^2 (Figure 4).

4.3. Active Erosional Processes

Examination of the extensive series of aerial photograms and historical orthoimages available for this area in the SDI-Canarias (GRAFCAN S.A., Canary Islands Government), revealed the occurrence of at least five decametric detachments on the sidewalls of *la barra* in the last 68 years, from 1954 to 2022 (Figure 10). They add up to a rock loss of 698.5 m^2, with 43.1 m of cumulative retreat along 116 m. Between 1963 and 1975, a rockfall event occurred (UTM X.456990, Y.3113010), in which 150 m^2 of rock was detached, leading to a maximum linear retreat of 8.8 m over a north-facing ramp sidewall. The frame from 1974 is the first in which this rockfall was clearly visible. Between 1987 and 1998, two rockfalls also occurred on north-facing ramp sidewalls. The larger of these (UTM X.457105, Y.3113240), measuring 214 m^2, had a maximum linear retreat of 9.2 m; and the smaller (UTM X.4567042, Y.3113075), measuring 115 m^2, had a maximum linear retreat of 9.3 m. The frames from 1989 and 1996 are, respectively, the first in the series in which they were clearly visible. The last two rockfalls occurred on west-facing erosional walls. The first (UTM X.457150, Y.3113270) occurred between 2004 and 2007 and affected 70 m^2 of rock mass with a maximum retreat of 6.8 m; and the second (UTM X.457010, Y.3113020) occurred between 2017 and 2019, and affected 145 m^2 of rock mass, leading to a linear retreat of 9.0 m. These collapses were first observed in the frames from 2007 and 2019, respectively.

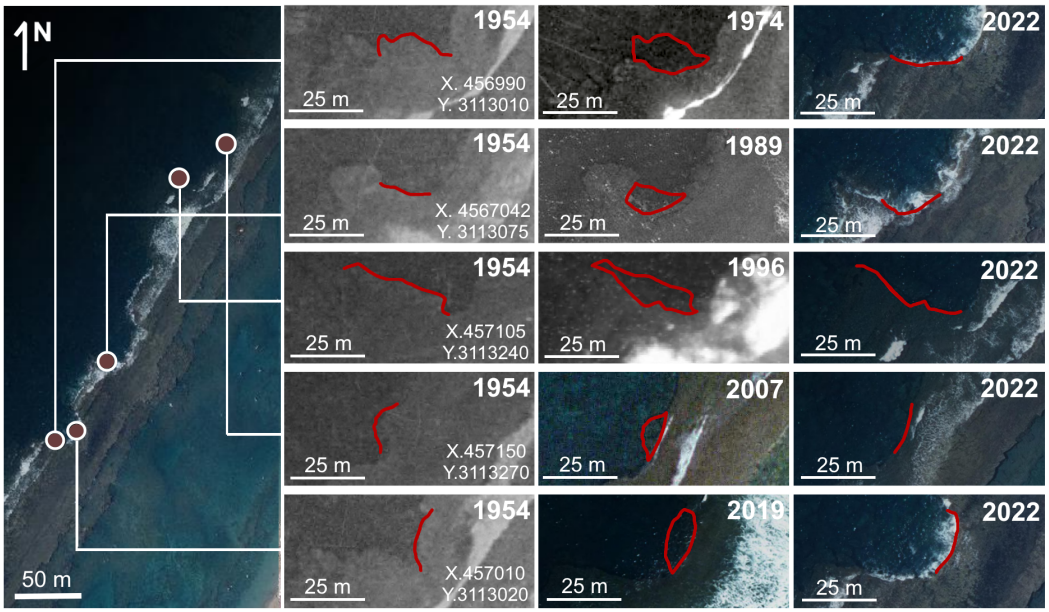

Figure 10. Rock areas eroded over the last 68 years (1954–2022) on the sidewalls of *la barra*, identified from the 22 historical aerial photographs and 18 digital orthophotos of the SDI-Canarias (GRAFCAN S.A., Canary Islands Government). The central column displays the first frames of the historical series in which the rock detachment is clearly visible. The red lines show the contours of the rocky edges. X,Y coordinates are metric units of the WGS84-UTM28N system.

5. Discussion

According to the geomorphological indicators found in the topo-bathymetric digital model and in the verifications carried out in situ, the current configuration of *la barra* must be interpreted as a rocky structure partially dismantled by natural and anthropic erosive processes. The interpretation of the results also leads to an estimation of the probable magnitude, patterns and rates of this disintegration over time.

While the natural erosional processes have mainly taken place at the front of the rocky structure, due to marine erosion, the erosional processes of human origin linked to the mining activities that took place centuries ago, are evident on its inner margin. According to Pérez-Torrado et al. [59], the extracted stone was mainly used as filters to remove water impurities thanks to the purification capacity of this sandstone rock. The reconstruction of the surface, according to high-resolution topo-bathymetry, had allowed to calculate the volume of calcarenite extraction at approximately 14,290 m^3; a value very close to the 15,000 m^3 estimated in previous field measurements [60].

The geomorphological configuration of the outer edge of the reef and the adjacent seabed provides new data to determine the spatio-temporal magnitude and mechanisms of marine erosion acting on *la barra*. The height of the bordering escarpment along the entire outer reef correlates with its planview morphology: the rocky headlands end in smaller escarpments than the rocky inlets, which form steep concavities where the highest falls are found. This difference in height-morphology is indicative of differential erosion processes and contrasting degrees of current retreat along the erosional frontal wall of the reef. In addition, the existence of an extensive submarine blockfield, extending up to 150 m from the outer edge of *la barra* (Figure 3c), more strongly supports the course of an extensive process of rock leveling due to prolonged marine erosion.

In this sector of the coastline of the island of Gran Canaria known as Confital Bay, the island shelf is approximately 4 km wide and has maximum depths below −100 m [61]. The blockfield of *la barra* de Las Canteras is mainly developed on a nearshore seabed of −5 to −10 m depth. It therefore extends over the inner sector of the island shelf that has been subjected to repeated flooding and emersion over geological time, due to Quaternary marine sea-level oscillations [62,63]. The sandstone blocks covering this surface are chaotically arranged and are of medium and large size, especially those covering the seabed adjacent to the intertidal rocky reef (Figures 5, 8 and 9).

Direct observation of historical rockfalls on the reef front, places the origin of the submarine blockfield by analogy to the present day in the disintegration of *la barra* by prolonged wave action, and the successive and numerous collapses of the outer wall. Examination of the historical series of aerial images available reinforces this position (Figure 10). The present day observations are consistent with the geomorphological indicators found in the topo-bathymetric digital model and shows that the erosion of *la barra* is mainly produced by large episodic rockfalls. Most of the detached blocks distributed on the closest outer seabeds are between 5 and 125 m^2 (Figure 9), while the five detachments detected in the historical period, since the middle of the 20th century, involve the uprooting of surfaces of more than 100 m^2, 20 m longitudinal wall lengths, and retreats of up to 9 m (Figure 10). They have occurred at north-facing points of ramps sidewalls or at west-facing points of inner walls of the erosive concavities. The frequency of this events over the last 68 years allows us to estimate an approximate return period of almost 14 years. However, this calculation may be underestimating the actual mean recurrence of smaller rockfalls, as observations are limited in time and constrained by the resolution and georeferencing quality of aerial imagery. Considering the total intertidal surface above −1 m depth, except for terrains degraded by extractions, the total detachment of 698.5 m^2 represents a loss over the last 68 years of 1.6% of the reef; an annual a rate of 0.02%/year.

The results indicate that rockfalls triggered by storm-wave impact are the primary erosion mode on *la barra.* Chemical and biological weathering processes are expected to act secondarily at a micro-scale, weakening the rocks and preparing them for mechanical wave erosion. The presence of small sandbanks in the nearshore blockfield enables wave

abrasion and may explain the development of rill-erosion morphologies on the intertidal reef ramps (Figure 7b).

The wave exposure and the pattern of discontinuities in the calcareous sandstone strata must determine the spatial distribution of the erosion in *la barra*, as is usual in these types of rocky coasts [38,64,65]. The distribution of historical rockfalls is consistent with the morphologies of the erosional front, as they occurred preferentially in pre-existing concavities (Figure 10). The concavities must be interpreted as incipient cross-shore erosional corridors that will ultimately fragment the reef longitudinally. Up to five in-progress erosional corridors can be observed today on *la barra grande* (Figures 6 and 10). Considering the strong influence of discontinuities on the patterns of coastal erosion in sedimentary rocks [38,64,65], the formation of these corridors may reflect the structural control of a set of discontinuities of NW–SE direction, which is also consistent with the dominant swell in this coastal sector. In turn, the northern orientation of some of the rockfalls suggests another direction of retreat, according to a possible NNE–SSW pattern of structural discontinuities, parallel to the planview layout of the reef and orthogonal to the NW–SE set of discontinuities. The topo-bathymetric model shows alignments consistent with this NNE–SSW retreat pattern in the disposition of the erosional submarine remnants (Figure 4).

The slight general NW tilt of the surface of *la barra* de Las Canteras is the topographic reflection of a seaward-dipping stratification, resulting from its paleo-coastal sedimentary origin [8,9,59]. These slopes, which are approximately 5º in the intertidal ramps, would have an essentially structural nature as a result of the cementation of an ancient beach formation (beachrock). The offshore projection of the slopes of the intertidal ramps in the topo-bathymetric digital model, links coherently with the series of submarine pinnacles detected at distances of between 50 and 100 m from the outer edge of *la barra*. They have flat surfaces of more than 100 m^2, also slightly tilted to the NW. This reinforces the interpretation of these submarine pinnacles as preserved erosional remnants of *la barra* (as 'sea stacks' on rocky cliffed coasts), which indicate former positions of the erosional front (see topo-bathymetric profiles 1, 2 and 3 in Figure 6). Together with the blockfield identified, the existence of these preserved remnants allows projection of the original extension of *la barra* up to an average distance of 150 m from the current outer edge. Bearing in mind that, at present, the average intertidal width of *la barra grande* is between 50 m and 100 m, depending on sectors, we currently witness a retreating of about 1/3 to 2/3 of the original rocky structure.

Stratigraphic studies have traditionally suggested that *la barra* was formed in the Last Interglacial period (MIS5e), approximately 110 ka ago, in an intertidal or subtidal coastal sedimentary environment [10]. Further cementation and consolidation of *la barra* into a calcarenite rock would probably have occurred during the marine regression. In the Last Glacial Period, the sea level dropped to the edge of the island shelf to more than −100 m depth [66]. Paleontological evidences indicate that the sea level remained up to two meters above present-day sea level in much of the Middle and Upper Holocene in the low-latitude Northeastern Atlantic region [67–69]. Considering that the erosional extension observed in the high-resolution topo-bathymetry is mostly between −5 and −10 m depth, the erosive capacity of waves on the subtidal sandstones would have been very limited since the positioning of the sea level at or above present-day levels 6500 years ago. As the most likely hypothesis, we would date the erosion of most of the subtidal structure of *la barra* in an earlier period, between 9000 and 6500 years B.P. (Lower and Middle Holocene), when the rising sea level transited from depths of −10 m to the present level. Since then (6500 years ago to the present), with different degrees of effectiveness depending on the metric variability of the Holocene mean sea levels [69], the erosion of the current intertidal rocks would have begun, observable as an active process at present (Figure 10). However, this interpretation should be cautiously considered, as recent studies dated similar beachrocks outcrops at Las Canteras beach to the Holocene transgression [9,70], which would place the formation and erosion processes of *la barra* much closer together in time.

6. Conclusions

Sandstone reefs are highly effective protective barriers against coastal erosion and safeguard the sedimentary stability of many sandy beaches. For this reason, *la barra* de Las Canteras is a natural coastal sandstone reef of great social and ecological value for the Canary Islands. Due to the apparent resistance of the rocks to the force of the waves and the relative slowness of the erosive processes, insufficient efforts have been made so far to know the magnitude, rate and form of the past and present erosion in *la barra*.

By means of high-resolution topo-bathymetry, obtained by combining different remote sensing technologies (echosounder, GPS and hyperspectral sensor), this work has provided new data to interpret features of its original configuration and its spatio-temporal evolution.

According to the geomorphological evidence provided in this paper, the original width of that sedimentary formation, which today is between ~50 and ~100 m (depending on the degree of erosion by sectors), could have been up to 200 m. The main hypothesis is that the erosional retreat of the sandstone reef occurred during the Holocene sea level rise. The erosion of the subtidal rocky structure of *la barra*, converted into a field of rockfall blocks below −5 m asl, together with the erosional semi-preserved remnants visible in the present topo-bathymetry, could be attributed to the transient eustatic rise from the Lower to the Middle Holocene. The erosion of the intertidal rocky masses (i.e., the intertidal platforms and ramps on whose walls active erosions are observed at present) would have occurred since the positioning of the sea at the present level, or up to 2 m above it in some time phases, about 6500 years ago.

The underwater and subaerial geomorphology of the reef shows how erosion follows preferential lines conditioned by wave exposure and, most probably, the geometry of an orthogonal fracture system. Differential erosion on the transverse fractures leads to the formation of concavities, the development of transverse erosional corridors (NW-SE) and, ultimately, the longitudinal fragmentation of *la barra grande.* Therefore, the erosive disintegration of the reef is marked by a process of fragmentation into pieces, as can be seen today in the different fragments of *la barra* along Las Canteras beach (*barra grande* and *barra amarilla*). At the same time, the likely exploitation of the longitudinal fracture lines produces a parallel retreat vector (NNE–SSW) which is concentrated on the north-facing walls of the intertidal rocky ramps. This can be seen in the present-day rockfalls and as is coherently attested to by the marked NNE–SSW dispositions of the subtidal erosional remnants found in the topo-bathymetric model.

At present, the erosion of *la barra* is a slow process marked by episodic collapses with an average frequency of almost 14 years, with up to 100 m^2 of rock mass losses and sudden retreats of 10 m on the outer edge of the reef. Over the past 68 years, 1.6% of the reef's preserved surface has been eroded; a low rate of 0.02%/year. However, it can be expected that the development of erosional corridors and the gradual loss of volume in *la barra grande* may lead to significant modifications of the waves and sea currents regime in the near future, even before its complete disintegration. It is therefore necessary to further investigate the erosional processes of *la barra* de Las Canteras, combining geomorphological monitoring techniques with hydrodynamic modelling, in order to project likely future scenarios and predict their ecological, cultural and economic consequences.

Author Contributions: Conceptualization, N.F.; Methodology, N.F. and K.S.; Software, K.S. and J.M.; Validation, K.S. and J.M.; Formal analysis, N.F.; Investigation, N.F.; Resources, J.V.; Data curation, N.F. and J.M.; Writing—original draft, N.F.; Writing—review & editing, K.S., J.M., J.V. and O.B.; Project administration, O.B.; Funding acquisition, O.B. All authors have read and agreed to the published version of the manuscript.

Funding: This research is a result of the project 'Evaluación de la capacidad de usos de La Barra de Las Canteras, considerando especies catalogadas y hábitats de la Red Natura 2000', co-funded by the Regional Ministry of Territorial Policy, Sustainability and Security (Government of the Canary Islands) and the European Regional Development Fund (ERDF) program 'Canarias Avanza con Europa'. Nicolás Ferrer is a beneficiary of the Postdoctoral contract programme 'Catalina Ruiz,

2021′ (APCR2021010018/6431001) co-funded by the Canary Islands Government and the European Social Fund.

Data Availability Statement: Not applicable.

Conflicts of Interest: The authors declare no conflict of interest.

References

1. Guimarães, T.; Mariano, G.; Barreto, A.; Sá, A.A. Beachrocks of Southern Coastal Zone of the State of Pernambuco (Northeastern Brazil): Geological resistance with history. *Geoheritage* **2017**, *9*, 111–119. [CrossRef]
2. Soares, M.D.O.; Rossi, S.; Martins, F.A.S.; Carneiro, P.B.D.M. The forgotten reefs: Benthic assemblage coverage on a sandstone reef (Tropical South-western Atlantic). *J. Mar. Biol. Assoc. UK* **2017**, *97*, 1585–1592. [CrossRef]
3. Darwin, C. On a remarkable bar of sandstone off Pernambuco, on the coast of Brazil. *Lond. Edinb. Dublin Philos. Mag. J. Sci.* **1841**, *19*, 257–260. [CrossRef]
4. Mabesoone, J.M. Origin and age of the sandstone reefs of Pernambuco (Northeastern Brazil). *J. Sedim. Res.* **1964**, *34*, 715–726. [CrossRef]
5. Chaves, N.S.; Sial, A.N. Mixed oceanic and freshwater depositional conditions for beachrocks of Northeast Brazil: Evidence from carbon and oxygen isotopes. *Int. Geol. Rev.* **1998**, *40*, 748–754. [CrossRef]
6. Pereira, L.S.; de Carvalho, D.M.; da Cunha, L.S. Methodology for the semi-quantitative evaluation of geoheritage applied to coastal geotourism in João Pessoa (Paraíba, Northest Brazil). *Geoheritage* **2019**, *11*, 1941–1953. [CrossRef]
7. Da Silva, M.L.N.; do Nascimento, M.A.L. Ecosystem services and typology of urban geodiversity: Qualitative assessment in Natal town, Brazilian Northeast. *Geoheritage* **2020**, *12*, 57. [CrossRef]
8. Alonso, I. North coast: Las Canteras beach. In *Tendencias Actuales en Geomorfología Litoral*; Hernández-Calvento, L., Alonso, I., Mangas, J., Yanes, A., Eds.; University of Las Palmas de Gran Canaria: Las Palmas de Gran Canaria, Spain, 2005; pp. 219–238.
9. Menéndez, I.; Herrera-Holguín, C.; Mangas, J. Upper Quaternary coastal palaeoenvironments and palaeosea levels in Las Canteras beach, Gran Canaria (Canary Islands, Spain). *Mar. Geol.* **2020**, *429*, 106322. [CrossRef]
10. Pérez-Torrado, F.J.; Mangas, J. Origin and geological evolution of the Las Canteras bar (Las Palmas de Gran Canaria). *Vector Plus* **1994**, *1*, 4–13.
11. Balcells, R.; Barrera-Morate, J.L.; Ruiz, M.T. Geological map of sheet 1101-I-II, scale 1:25,000. (Las Palmas de Gran Canaria). In *Memoir*; ITGE: Madrid, Spain, 1990; p. 131.
12. Meco, J.; Petit-Maire, N.; Fontugne, M.; Shimmield, G.; Ramos, A.J. The Quaternary deposits in Lanzarote and Fuerteventura (Eastern Canary Islands, Spain): An overview. In *Climates of the Past. Proceeding CLIP Project*; Meco, J., Petit-Maire, N., Eds.; Universidad de Las Palmas de Gran Canaria (ULPGC): Las Palmas, Spain, 1997; pp. 123–136.
13. Eversole, D.; Fletcher, C.H. Longshore sediment transport rates on a reef-fronted beach: Field data and empirical models Kaanapali Beach, Hawaii. *J. Coast. Res.* **2003**, *19*, 649–663.
14. Bosserelle, C.; Gallop, S.L.; Haigh, I.D.; Pattiaratchi, C.B. The influence of reef topography on storm-driven sand flux. *J. Mar. Sci. Eng.* **2021**, *9*, 272. [CrossRef]
15. Trenhaile, A. Rocky coasts—their role as depositional environments. *Earth Sci. Rev.* **2016**, *159*, 1–13. [CrossRef]
16. Gallop, S.L.; Kennedy, D.M.; Loureiro, C.; Naylor, L.A.; Muñoz-Pérez, J.J.; Jackson, D.W.; Fellowes, T.E. Geologically controlled sandy beaches: Their geomorphology, morphodynamics and classification. *Sci. Environ.* **2020**, *731*, 139123. [CrossRef]
17. Muñoz-Pérez, J.J.; Tejedor, L.; Medina, R. Equilibrium beach profile model for reef-protected beaches. *J. Coast. Res.* **1999**, *15*, 950–957.
18. Gallop, S.L.; Bosserelle, C.; Eliot, I.; Pattiaratchi, C.B. The influence of limestone reefs on storm erosion and recovery of a perched beach. *Cont. Shelf Res.* **2012**, *47*, 16–27. [CrossRef]
19. Gallop, S.L.; Bosserelle, C.; Eliot, I.; Pattiaratchi, C.B. The influence of coastal reefs on spatial variability in seasonal sand fluxes. *Mar. Geol.* **2013**, *344*, 132–143. [CrossRef]
20. Rodríguez-Padilla, I.; Castelle, B.; Marieu, V.; Morichon, D. Video-Based Nearshore Bathymetric Inversion on a Geologically Constrained Mesotidal Beach during Storm Events. *Remote Sens.* **2022**, *14*, 3850. [CrossRef]
21. Alonso, I.; Vilas, F. The influence of boundary conditions on beach zonation. In *Coastal Dynamics*; ASCE: Reston, VA, USA, 1994; pp. 417–431.
22. Jackson, D.W.T.; Cooper, J.A.G.; Del Rio, L. Geological control of beach morphodynamic state. *Mar. Geol.* **2005**, *216*, 297–314. [CrossRef]
23. Dugan, J.P.; Morris, W.D.; Vierra, K.C.; Piotrowski, C.C.; Farruggia, G.J.; Campion, D.C. Jetski-based nearshore bathymetric and current survey system. *J. Coast. Res.* **2001**, *17*, 900–908.
24. Maleika, W.; Palczynski, M.; Frejlichowski, D. Interpolation methods and the accuracy of bathymetric seabed models based on multibeam echosounder data. In Proceedings of the Intelligent Information and Database Systems: 4th Asian Conference, ACIIDS 2012; Proceedings, Part III 4, Kaohsiung, Taiwan, 19–21 March 2012; Springer: Berlin/Heidelberg, Germany, 2012; pp. 466–475.
25. Stockdon, H.F.; Holman, R.A. Estimation of wave phase speed and nearshore bathymetry from video imagery. *J. Geophys. Res. Oceans* **2000**, *105*, 22015–22033. [CrossRef]

26. Lee, Z.; Carder, K.L.; Mobley, C.D.; Steward, R.G.; Patch, J.S. Hyperspectral remote sensing for shallow waters: 2. Deriving bottom depths and water properties by optimization. *Appl. Opt.* **1999**, *38*, 3831–3843. [CrossRef]
27. Lyzenga, D.R.; Malinas, N.P.; Tanis, F.J. Multispectral bathymetry using a simple physically based algorithm. *IEEE Trans. Geosci. Remote Sens.* **2006**, *44*, 2251–2259. [CrossRef]
28. Ferrario, F.; Beck, M.W.; Storlazzi, C.D.; Micheli, F.; Shepard, C.C.; Airoldi, L. The effectiveness of coral reefs for coastal hazard risk reduction and adaptation. *Nat. Commun.* **2014**, *5*, 1–9. [CrossRef]
29. Gallop, S.L.; Young, I.R.; Ranasinghe, R.; Durrant, T.H.; Haigh, I.D. The large-scale influence of the Great Barrier Reef matrix on wave attenuation. *Coral Reefs* **2014**, *33*, 1167–1178. [CrossRef]
30. Robinson, L.A. Erosive processes on the shore platform of northeast Yorkshire, England. *Mar. Geol.* **1977**, *23*, 339–361. [CrossRef]
31. Bird, E.C. *Coastal Geomorphology: An Introduction*; John Wiley & Sons: Hoboken, NJ, USA, 2008.
32. Gill, E.D.; Lang, J.G. Micro-erosion meter measurements of rock wear on the Otway coast of southeast Australia. *Mar. Geol.* **1983**, *52*, 141–156. [CrossRef]
33. Stephenson, W.J.; Kirk, R.M.; Hemmingsen, S.A.; Hemmingsen, M.A. Decadal scale micro erosion rates on shore platforms. *Geomorphology* **2010**, *114*, 22–29. [CrossRef]
34. Stephenson, W.J.; Kirk, R.M.; Kennedy, D.M.; Finlayson, B.L.; Chen, Z. Long term shore platform surface lowering rates: Revisiting Gill and Lang after 32 years. *Mar. Geol.* **2012**, *299*, 90–95. [CrossRef]
35. Trenhaile, A.S.; Porter, N.J. Shore platform downwearing in eastern Canada; A 9–14 year micro-erosion meter record. *Geomorphology* **2018**, *311*, 90–102. [CrossRef]
36. Stephenson, W.J.; Naylor, L.A. Geological controls on boulder production in a rock coast setting: Insights from South Wales, UK. *Mar. Geol.* **2011**, *283*, 12–24. [CrossRef]
37. Naylor, L.A.; Stephenson, W.J.; Smith, H.C.; Way, O.; Mendelssohn, J.; Cowley, A. Geomorphological control on boulder transport and coastal erosion before, during and after an extreme extra-tropical cyclone. *Earth Surf. Process. Landf.* **2016**, *41*, 685–700. [CrossRef]
38. Buchanan, D.H.; Naylor, L.A.; Hurst, M.D.; Stephenson, W.J. Erosion of rocky shore platforms by block detachment from layered stratigraphy. *Earth Surf. Process. Landf.* **2020**, *45*, 1028–1037. [CrossRef]
39. Trenhaile, A.S. *The Geomorphology of Rock Coasts*; Clarendon Press: Oxford, UK, 1987; Volume 1168.
40. Trenhaile, A.S. Modeling the development of wave-cut shore platforms. *Mar. Geol.* **2000**, *166*, 163–178. [CrossRef]
41. Walkden, M.J.A.; Hall, J.W. A predictive mesoscale model of the erosion and profile development of soft rock shores. *Coast. Eng.* **2005**, *52*, 535–563. [CrossRef]
42. Thébaudeau, B.; Trenhaile, A.S.; Edwards, R.J. Modelling the development of rocky shoreline profiles along the northern coast of Ireland. *Geomorphology* **2013**, *203*, 66–78. [CrossRef]
43. Alonso, I. Sedimentary Processes at Las Canteras Beach (Gran Canaria). Ph.D. Thesis, University of Las Palmas de Gran Canaria, Las Palmas de Gran Canaria, Spain, 1993.
44. Arriola-Velásquez, A.; Tejera, A.; Guerra, J.G.; Alonso, I.; Alonso, H.; Arnedo, M.A.; Martel, P. Spatio-temporal variability of natural radioactivity as tracer of beach sedimentary dynamics. *Estuar. Coast. Shelf Sci.* **2019**, *231*, 106476. [CrossRef]
45. Alonso, I.; Vilas, F. Sedimentary variability at Las Canteras beach (Gran Canaria). *Geogaceta* **1996**, *20*, 428–430.
46. Martínez-Martínez, J.; Gordo Rojas, M.C.; Santana, J.M.; Jiménez, J.A.; Veloso Quevedo, J.J. Sedimentary dynamics at Las Canteras beach (Las Palmas de Gran Canaria). *Rev. Obras Públ.* **1988**, *2*, 145–152.
47. Martínez-Martínez, J.; Álvarez Espejo, R.; Bilbao, I.A.; Rodríguez Cabrera, R. Analysis of sedimentary processes on the Las Canteras beach (Las Palmas, Spain) for its planning and management. *Eng. Geol.* **1990**, *29*, 377–386. [CrossRef]
48. Alonso, I. Spatial beach morphodynamics. An example from Canary Islands, Spain. *Litoral* **1994**, *94*, 169–183.
49. Alonso, I. Medición del transporte de sedimentos por olas y corrientes. *Vector Plus Sci. Cult. Misc.* **1999**, *14*, 13–23.
50. Sánchez García, M.J.; Casamayor Font, M.; Alonso Bilbao, I.; Rodriguez, S. Long-term evolution of the coastline at Las Canteras beach (Canary Islands). *Geotemas* **2015**, *15*, 85–88.
51. Tuya, F.; Asensio, M.; Bosch, N.E.; García, A.; Navarro, A. Partitioning multiple diversity dimensions of nearshore fish assemblages within a coastal seascape. *Hydrobiologia* **2019**, *834*, 87–102. [CrossRef]
52. Tuya, F.; Asensio, M.; Navarro, A. "Urbanite" rays and sharks: Presence, habitat use and population structure in an urban semi-enclosed lagoon. *Reg. Stud. Mar. Sci.* **2020**, *37*, 101342. [CrossRef]
53. Martin, J.; Eugenio, F.; Marcello, J.; Medina, A. Automatic sun glint removal of multispectral high-resolution WorldView-2 imagery for retrieving coastal shallow water parameters. *Remote Sens.* **2016**, *8*, 37. [CrossRef]
54. Guillemot, C.; Le Meur, O. Image inpainting: Overview and recent advances. *IEEE Signal Process. Mag.* **2013**, *31*, 127–144. [CrossRef]
55. Zhonping, L. Hyperspectral remote sensing for shadow waters: 2. Deriving bottom depths and water properties by optimization. *Appl. Opt.* **1999**, *38*, 18.
56. Gavin, H.P. *The Levenberg-Marquardt Method for Nonlinear Least Squares Curve-fitting Problems*; Department of Civil and Environmental Engineering, Duke University Durham: Durham, NC, USA, 2013.
57. Hobson, R.D. Surface Roughness in Topography: A Quantitative Approach. In *Spatial Analysis in Geomorphology*; Chorley, R.J., Ed.; Harper & Row: London, UK, 1972; pp. 221–245.

58. Sappington, J.M.; Longshore, K.M.; Thomson, D.B. Quantifying Landscape Ruggedness for Animal Habitat Analysis: A case Study Using Bighorn Sheep in the Mojave Desert. *J. Wildl. Manag.* **2007**, *71*, 1419–1426. [CrossRef]
59. Pérez-Torrado, F.J.; Cabrera, M.C.; Hansen Machín, A.; Rodriguez-Gonzalez, A. *Geolodía 13 Gran Canaria: An Urban Geological Walk*; Las Palmas de Gran Canaria: Las Palmas, Spain, 2013.
60. Otero Paz, I. *La Historia de Las Palmas de Gran Canaria, Enterrada en la Playa de Las Canteras*; elDiario.es: Las Palmas de Gran Canaria, Spain, 2016. Available online: https://www.eldiario.es/canariasahora/cultura/palmas-gran-canaria-enterrada-canteras_1_4042039.html (accessed on 20 April 2023).
61. Instituto Español de Oceanografía. *Topobathymetric Map of the Canary Islands 1:700,000 (UTM 28N Ellipsoid WGS84 Projection)*; Instituto Español de Oceanografía, Ministerio de Educación y Ciencia: Madrid, Spain, 2006; ISBN 84-958-77-30-9.
62. Meco, J.; Guillou, H.; Carracedo, J.C.; Lomoschitz, A.; Ramos, A.J.G.; Rodríguez-Yánez, J.J. The maximum warmings of the Pleistocene world climate recorded in the Canary Islands. *Palaeogeogr. Palaeoclimatol. Palaeoecol.* **2002**, *185*, 197–210. [CrossRef]
63. Zazo, C.; Goy, J.L.; Hillaire-Marcel, C.; Gillot, P.Y.; Soler, V.; Gonzalez, J.Á.; Ghaleb, B. Raised marine sequences of Lanzarote and Fuerteventura revisited-a reappraisal of relative sea-level changes and vertical movements in the eastern Canary Islands during the Quaternary. *Quat. Sci. Rev.* **2002**, *21*, 2019–2046. [CrossRef]
64. Kennedy, D.M.; Dickson, M.E. Lithological control on the elevation of shore platforms in a microtidal setting. *Earth Surf. Process. Landf. J. Br. Geomorphol. Res. Group* **2006**, *31*, 1575–1584. [CrossRef]
65. Naylor, L.A.; Stephenson, W.J. On the role of discontinuities in mediating shore platform erosion. *Geomorphology* **2010**, *114*, 89–100. [CrossRef]
66. Rijsdijk, K.F.; Hengl, T.; Norder, S.J.; Otto, R.; Emerson, B.C.; Ávila, S.P.; López, H.; van Loon, E.; Tjørve, E.; Fernández-Palacios, J.M. Quantifying surface-area changes of volcanic islands driven by Pleistocene sea-level cycles: Biogeographical implications for the Macaronesian archipelagos. *J. Biogeogr.* **2014**, *41*, 1242–1254. [CrossRef]
67. Ballouche, A.; Lefevrè, D.; Carruesco, C.; Raynal, J.P.; Texier, J.P. Holocene environments of coastal and continental Morocco. In *Quaternary Climate in Western Mediterranean*; Lopez Vera, F., Ed.; Universidad Autónoma de Madrid: Madrid, Spain, 1986; pp. 517–531.
68. Barusseau, J.P.; Descamps, C.; Giresse, P.; Monteillet, J.; Pazdur, M. Nouvelle définition des niveaux marins le long de la côte nord-mauritienne (Sud du Banc d'Arguin) pendant les cinq derniers millénaires. *Comptes Rendus L'académie Sci. Sér. 2 Mécanique Phys. Chim. Sci. L'univers Sci. Terre* **1989**, *309*, 1019–1024.
69. Meco, J.; Lomoschitz, A.; Rodríguez, Á.; Ramos, A.J.; Betancort, J.F.; Coca, J. Mid and Late Holocene sea level variations in the Canary Islands. *Palaeogeogr. Palaeoclimatol. Palaeoecol.* **2018**, *507*, 214–225. [CrossRef]
70. Herrera-Holguín, A.C.; Menéndez, I.; Mangas, J. Beachrock, paleosuelo y aeolianita holocenas en el arco central de la playa de las canteras (NE de Gran Canaria, España). In Proceedings of the XV Reunión Nacional de Cuaternario Bizkaia Aretoa, Bilbao, Spain, 1–5 July 2019; Libro de Resúmenes; Universidad del País Vasco/Euskal Herriko Unibertsitatea: Leioa, Spain, 2019; pp. 243–246.

Disclaimer/Publisher's Note: The statements, opinions and data contained in all publications are solely those of the individual author(s) and contributor(s) and not of MDPI and/or the editor(s). MDPI and/or the editor(s) disclaim responsibility for any injury to people or property resulting from any ideas, methods, instructions or products referred to in the content.